Journal of Thermal Analysis and Calorimetry, Vol. 90 (2007) 1, 107–113

RATIONAL MECHANOCHEMICAL PROCESSES WITH LESS INTENSIVE STRESSING FOR THEIR AFFORDABLE APPLICATION

M. Senna[*]

Faculty of Science and Technology, Keio University, Yokohama, 223-8522, Japan

An overview is given on the application of mechanical activation to various fields of solid state processes. Opposite to the historical development, emphasis is laid to give mechanical energy as sparingly as possible to the point where mechanical stressing is indispensable. Case studies were demonstrated in three different genres, i.e., organic synthesis, electroceramics and utilization of mineral resources.

Keywords: *charge transfer, Diels-Alder reaction, electroceramics, mechanochemistry, wolframate*

Introduction

In the era of fast developing technologies in nanocomposites with various new functions under simultaneous environmental restrictions, mechanochemical processes need to be reconsidered to adapt these seemingly self-contradictory requirements. One of the most important items is obviously to invest as minimal external energy as possible, since mechanical activation is energetically inefficient and hence expensive. On the other hand, there are several steps which mechanical stressing can realize far better than any other processes. After being deeply influenced from a number of outstanding books [1–7], the present author has also tried to summarize related issues [8–14]. Still smarter mechanochemical processes are explored in the present overview, to adapt the contemporary requirements mentioned above.

Although mechanochemistry was considered to be a branch of inorganic solid state chemistry due to its historical reasons, molecular crystals turned out to be more sensitive to mechanical stressing and hence research works in this area are increasing [15–21]. Chemical interactions between organic species like amino acids and metals are understood under the concept of coordination, where the charge transfer between the metal and the ligands play a principal role [10]. This kind of interaction can open a new way to ceramics processing [22, 23].

Importance of forced symmetry breakage and intimate contact between dissimilar species under mechanical stressing is to be emphasized [15]. For those purposes, energy density is not of primary importance. Instead, other more subtle items such as timing of stressing, environment or coexisting species play more important roles. Another viewpoint is better utilization of resources by rational use of mechanical stressing [24, 25].

Explicit case studies based on our own research works are exhibited from organic syntheses, materials for microelectronics to direct synthesis of nano-structured materials from natural resources, under the unified motto of rationalization of mechanochemistry.

Organic syntheses

One of the major obstacles for a solid state reaction is the restricted number of reaction fronts, i.e. only at the inter-particulate contact points between dissimilar reactant species. In a solid state host-guest complex, however, a large number of molecules could be tied up by non-covalent bonding leady to form host-guest complexes. A simple example is a charge transfer complex (CTC) between hydroquinone (electron donor) and benzoquinone (electron acceptor) [26, 27]. Phenols [28, 29], naphthols [30, 31] or 1-1'-bi-2-naphthol (BINOL) [32–34] can serve as an electron donor. In the case of BINOL, aromatic compounds such as benzene and anthracene are incorporated into the crystalline network of CTC between BQ and BINOL. This kind of composite crystal is formed directly in a solid-state process [32].

A Diels–Alder reaction starting from a stoichiometric solid mixture of dimethylanthracene (DMA) and *p*-benzoquinone (BQ) was efficiently catalyzed by adding a small amount of phenol derivatives via autogenous formation of eutectic complexes [35]. The main mechanisms for the formation of eutectic complex with hydrogen bonds were the inter-

* senna@applc.keio.ac.jp

1388–6150/$20.00

Akadémiai Kiadó, Budapest, Hungary
Springer, Dordrecht, The Netherlands

position of the charge transfer from a phenol to a quinone under the influence of steric hindrance by alkyl groups introduced into phenols [36]. Some of the key issues with extracted experimental procedures are reproduced below.

An equimolar mixture (typically 1 mmol, each) of crystalline powders of derivatives of phenol and quinone were mixed in an agate mortar with a pestle in ambient atmosphere at 298 K. We used cresol (CR), thymol (TM) or 3-*tert*-butylphenol (TBP) as a phenol and *p*-benzoquinone (BQ), methyl-*p*-benzoquinone (MeBQ) and *tert*-butyl-*p*-benzoquinone (TBBQ) as a quinone. Crystalline powders of a phenol and a quinone in a stoichiometric proportion were mixed in an agate mortar at an ambient condition. In many cases e.g. with TM and BQ, the powder mixture was turned to red liquid immediately after mixing.

Table 1 summarizes the state and color of the resulted complexes. When we use MeBQ or TBBQ as a quinone, all the combinations led to autogenous fusion with simultaneous color change into either dark red or light orange. When we use BQ as a quinone, mixtures with CR or TBP in the stoichiometric proportion turned their color into red to indicate the formation of CTCs, but remained in a solid state without autogenous fusion. On the other hand, combination of the BQ and TM at the molar ratio 1:2 resulted in an autogenous fusion to change into a red eutectic complex.

We then compared the systems BQ-TBP, which gave solid complex, and BQ-TM, as a eutectic complex, to examine the difference in the molecular interaction by virtue of IR spectra. Kubinyi *et al.* [37] reported that hydrogen bond formation leads to a red shift of C=O stretching band, while π-charge transfer interaction causes a red shift of the out-of-plane C–H deformation band. Indeed, C=O stretching band of BQ (1658 cm^{-1} in $CHCl_3$) was red shifted in the combinations BQ-TBP (by 15 cm^{-1} in a solid state) and BQ-TM (by 5 cm^{-1} in a eutectic state), respectively. From these results, we recognize that hydrogen bonds are also formed in the eutectic complex.

Table 1 States and colors of CTC with varying combinations

Quinone	Phenol	Molar ratio quinone:phenol	State	Color
BQ	CR	1:1	solid	red
BQ	TM	1:2	liquid	red
BQ	TBP	1:1	solid	red
MeBQ	CR	1:1	liquid	red
MeBQ	TM	1:1	liquid	red
MeBQ	TBP	1:1	liquid	red
TBBQ	CR	1:1	liquid	orange
TBBQ	TM	1:1	liquid	orange
TBBQ	TBP	1:1	liquid	orange

We further examined a Diels–Alder reaction in a eutectic complex medium. As a model reaction, we have chosen the reaction system between DMA and BQ. In the course of the reaction, viscosity of the reaction mixture increased, and the mixture completely solidified after 30 min to complete the reaction, as shown in Fig. 1. Effects of BINOL and TM on the rate of Diels–Alder reaction are quite obvious, as shown in Fig. 2.

Addition of a catalytic amount (10 mol%) of TM to the same reaction system was examined. The amount of the eutectic phase was very minute under this condition, so that the reaction mixture could be handled like a solid state reaction, to use a ball mill. By adding a stoichiometric amount of TM, 95% yield was obtained only in 30 min. The reaction was also fast with a catalytic amount of TM, i.e. 95% yield in 2 h. In the case of additives giving solid-state complexes, the yield was only moderate. This clearly

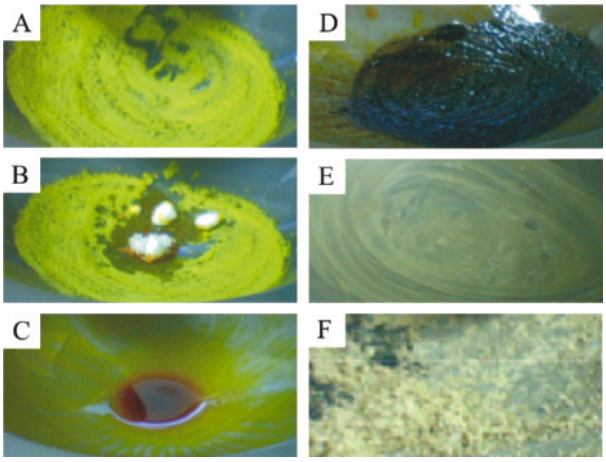

Fig. 1 Change in the appearance during autogenous fusion and CTC-catalyzed Diels–Alder reaction, A – BQ, B – just after the addition of CR, C – state of autohenous fusion, D – 1 min after DMA addition, E – 20 min after gentle mixing and F – state of reaction completion by gentle mixing for 30 min

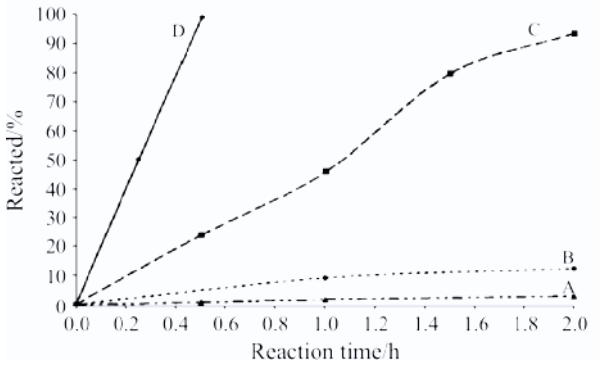

Fig. 2 Reaction kinetic curves of catalysed Diels–Alder reaction between BQ and DMA with different additives, i.e. A – none, B – 5 mol% BINOL, C – 10 mol% TM and D – 200 mol% TM

demonstrates that the reaction in a eutectic medium is much faster than those in a solid state complex. In addition, the reaction carried out in a solution gave moderate yields [35]. These results are explained by the absence of the hydrogen bonds in a solution.

By the reaction processes demonstrated above, sluggishness of the solid-state reaction is significantly eliminated. We also emphasize that simultaneous hydrogen bonding during the complex formation process furnishes additional merits of the present organic catalyses in solvent-free Diels–Alder reactions.

Electroceramics

Solid-state processes are advantageous over competing alternatives via solution of vapor phases to fabricate electroceramic materials due primarily to high productivity, cost merits and ecology. However, we have to overcome well known shortcomings of inhomogeneity i.e. low reactivity and associated necessity of high temperature often leading to disfavored grain growth. Well-dispersed, fine particulate raw materials are nowadays commercially available at a reasonable price, so that the main purpose of milling a mixture is shifted from size reduction and intensive mechanical activation to homogenization of the reaction mixture. Excessive mechanical activation is even hazardous, when we have to suppress grain growth. Appropriate choice of the starting species of cationic ingredients may not be underestimated either. Several case studies will be summarized below for representative ferroic materials.

PMN-PT

Starting from a stoichiometric mixture comprising respective oxides with an exception of $Mg(OH)_2$, being a stable hydroxide, instead of MgO, solid solutions of perovskite, $PbMg_{1/3}Nb_{2/3}O_3$ with $PbTiO_3$ (PMN-*x*PT with x=0, 0.1 or 0.2) were synthesized [38]. Increase in the microhomogeneity of the mixture was demonstrated in Fig. 3 by using the standard deviation of the local atomic ratio from the overall nominal one determined by EDX installed in the transmission electron microscope. The principle of this kind of homogeneity evaluation is identical with those adopted for the degree of mixing in a much larger scale [39].

Change in the electronic states of the mixture is then to be examined as a criterion of 'chemical homogeneity'. While change in the O1s by grinding is rather straightforward to near that of the final product [38], we also have more detailed discussion based on the change in the Nb3d XPS pattern. As shown in Fig. 4, partial reduction of Nb^{5+} to Nb^{2+} was detected. Difference in the DTA profile is also significant as shown in Fig. 5. While

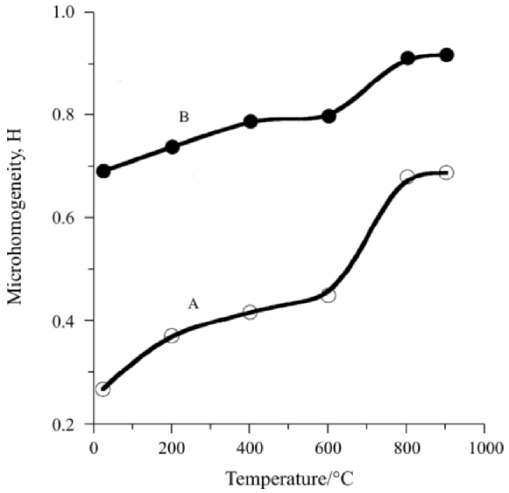

Fig. 3 Change in the microhomogeneity of the reaction system PMN-0.1PT by milling and heating with ca. 25 nm special resolution, evaluated by EDX installed in TEM; A – without milling and B – milling for 1 h

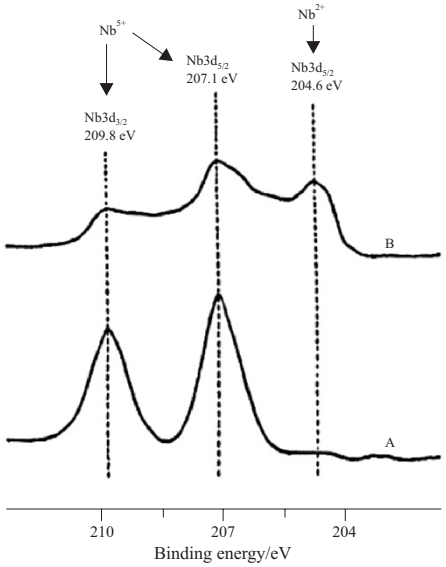

Fig. 4 XPS profiles of Nb3d for the reaction system PMN-0.1PT; A – without milling and B – milling for 1 h

endothermic peak due to dehydration of $Mg(OH)_2$ (peak 1) became much smaller for milled sample, decrease in the temperature of the exothermic peak due to pyrochlore formation was as large as ca. 100 K (from peak 3 to peak 2). Endothermic peak due to melting of PbO (peak 4) disappeared by milling. All these changes consistently indicate homogenization and incipient chemical reaction during milling.

This, together with the disappearance of the IR absorption from OH, mechanochemical dehydration and associated charge transfer are clearly demonstrated. These experimental findings backup the formation of bridging hetero-metalloxane bonds, being the fundamental principle of soft mechanochemistry [8].

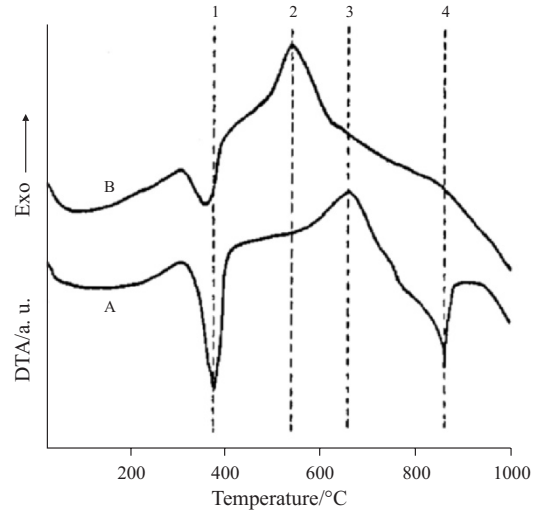

Fig. 5 DTA profiles for the reaction system PMN-0.1PT; A – without milling and B – milling for 1 h

As we calcined the mechanically homogenized mixtures mentioned in the previous section at 850°C for 4 h, we obtained always phase pure perovskite. Morphology of the calcined powders is also much more uniform when we started from homogenized mixture [38]. The lattice constant decreased linearly with x, indicating the formation of uniform PMN-PT solid solution. The obvious superiority of the mechanically pretreated products in the dielectric properties [38] is primarily attributed to the elimination of the second phase, pyrochlore.

$Ba(Mg_{1/3}Ta_{2/3})O_3$ (BMT)

In the case of $Ba(Mg_{1/3}Ta_{2/3})O_3$ (BMT), success of mechanical activation was only reached by using hydrated sample, $Ta_2O_5{\cdot}3.8H_2O$, in place of anhydrous Ta_2O_5 [40]. The second phase, $BaTi_2O_4$, was almost disappeared, if not completely, by using mechanically activated mixture with $Ta_2O_5{\cdot}3.8H_2O$. From the XPS analyses we recognized that the hydrated water was disappeared after milling [40]. We attributed this to the consumption of hydrated water due to the formation of bridging bonds, Ba–O–Ta and Mg–O–Ta, across the boundary of dissimilar particle species. It is particularly noteworthy by referring XPS profiles that the electronic state of the starting mixture becomes very close to that of well-crystallized BMT [40].

Ba-hexaferrites

Necessary conditions for the synthesis of phase pure Z-type hexagonal barium ferrite ($Ba_3Co_2Fe_{24}O_{41}$, Z-hex) are quite different from those mentioned above for various perovskite-related electroceramics. While mechanical activation works relatively straightforwardly for the syntheses of M-phase [41] and Y-phase [42] hexaferrites, phase pure synthesis of Z-phase is by far more difficult. A stoichiometric mixture for Z-hex composition was milled in water in a conventional rotational ball mill and dried at 100°C for 12 h, to obtain the starting mixture. We subsequently calcined the starting mixture at 1080°C for 2 h to obtain the intermediate, comprising M-type and Y-type hexaferrites. The intermediate was then dispersed in distilled water and milled with a planetary mill for 1 h. The slurry was dried and subsequently calcined for the second time at temperatures between 1180 and 1230°C for 2 h. The same intermediates were subjected to dry milling for comparison, under the same operational condition. While wet milling of the intermediate brought about Z-hex in an almost phase pure state (phase purity more than 90%), dry milling resulted in much lower extent of Z-hex [43, 44]. We attributed the success with intermediate wet milling to the preservation of the layered structure, as schematically represented in Fig. 6.

Better utility of natural resources toward high-valued material

Application of mechanical activation technology to natural resources, among others to mineral processing, has a long tradition. Starting materials of any high-valued materials are after all natural resources. However, little attempts were made to obtain high-valued nano-structured materials rather directly from mechanical activation. Here is an example where nanoparticles of WC or W were obtained from wolframate ($FeWO_4$). This was achieved by calcining mechanically activated mixtures of wolframite and carbon powders in Ar [45, 46]. Since high cost of WC production is attributed to a number of high temperature processes, reduction of processing temperature is of utmost importance. Until recently, only a small amount of reduction was observed at temperatures around 1200°C [47]. As a matter of fact, mechanical activation has been effectively used to prepare WC

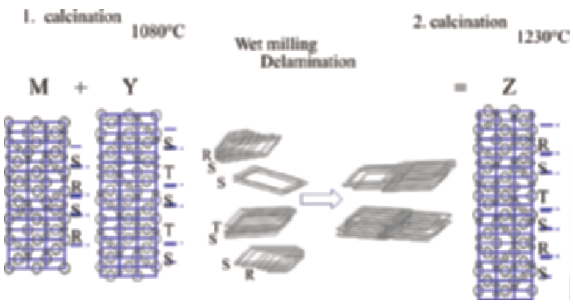

Fig. 6 Reaction schemes of Z-phase hexaferrite by two-step heating with delaminating wet milling on the intermediate

from a mixture comprising tungsten powder and activated carbon [48, 49]. We succeeded in directly synthesize WC from wolframite with the aid of mechanical activation [45, 46].

Natural wolframite was supplied from Bayan-Ulgii, western Mongolia. As carbon sources we used commercial active carbon or recycled graphite. The composition of the mixture was set equal to the stoichiometry of the reaction, $FeWO_4+5C\rightarrow Fe+WC+4CO$. Powder mixtures were mechanically activated by a planetary mill (Fritsch, Pulversitte 5) and uniaxially compressed into pellets. The pellets were calcined up to 1100°C under flowing Ar gas.

It is noteworthy that the mixture milled for 0.5 h (sample W-0.5) resulted in almost phase pure WC after calcining at 900°C, as shown in Fig. 7, while activation for 2 h (W-2) gave rise to a second phase, i.e. the ternary carbide Fe_6W_6C according to the reaction, $6FeWO_4+25C\rightarrow Fe_6W_6C+24CO$. Thermoanalytical profiles were compared in Fig. 8. A decrease of the endothermic peak temperature in W-2 is related with an increase in the rate of ternary carbide formation, as a consequence of the improved homogeneity. When we heat at 1100°C, sample W-0 did not react at all. Therefore, the mass loss and associated endothermic process in sample W-0 are most likely ascribed to the dissipation of remained carbon by reacting with the remaining trace of oxygen in the furnace.

Figure 9 displays a bright field transmission electron microphotograph taken from the sample W-2

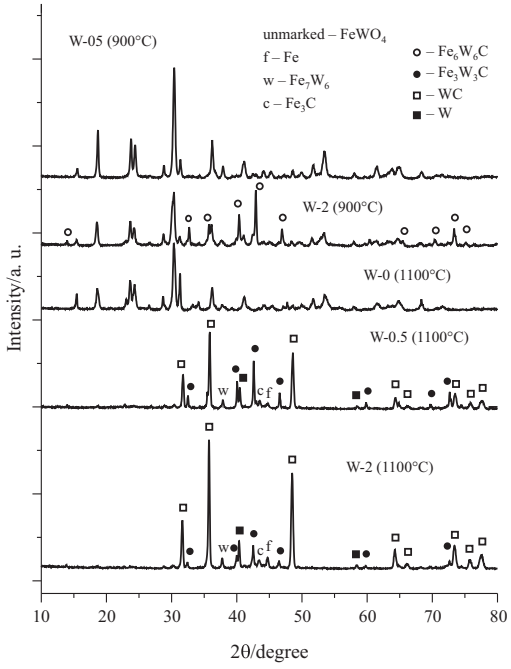

Fig. 7 X-ray diffractograms of the mixtures of $FeWO_4$ and active carbon calcined at varying temperatures. The value *n* in the sample description, W-*n* denotes milling time of the starting mixture in h

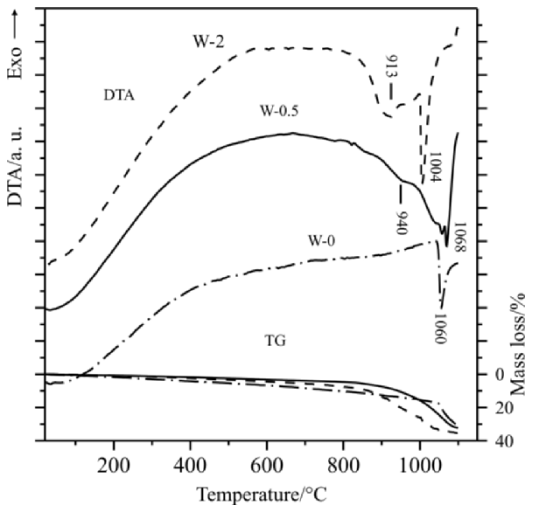

Fig. 8 TG-DTA profiles of the mixtures of $FeWO_4$ and active carbon. The value *n* in the sample description, W-*n* denotes milling time of the starting mixture in h

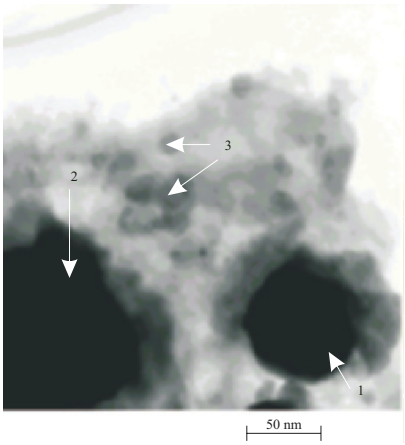

Fig. 9 Transmission electron microphotograph taken from sampleW-2 after heating at 1100°C. Large dark spots are $FeWO_4$ (arrow 1), ternary carbide particles, (arrow 2) surrounded by smaller WC particles (arrow 3)

after heating at 1100°C. We observe large dark wolframite (arrow 1) and ternary carbide particles (arrow 2) surrounded by smaller WC particles (arrow 3). We recognize the average particle size of WC to be around 20–25 nm, which agrees well with the crystallite size, 30 nm, determined from the XRD line broadening. This implies the nanoparticles we obtained in the present direct carbothermic reduction are WC single crystals.

WC formation is a diffusion-controlled process [47]. It is therefore obvious that milling the reacting mixture brings about its homogenization, an increase in the number of reacting contact points and a decrease in the diffusion path to ease the formation of ternary carbides and, finally that of WC without the formation of W_2C. Preparation of WC with higher purity from natural wolframite mineral still requires re-

finement and optimization of the milling and heating processes, apart from additional purification steps.

Similar mechanical activation and subsequent carbothermal reduction of tungstite ($WO_3 \cdot H_2O$) obtained from natural wolframite by acid leaching resulted in the tungsten nanoparticles [46] by the reaction scheme was $WO_3+3C \rightarrow WO_2+CO+2C \rightarrow W+3CO$. Fine-grained microstructure of the leached tungstite is the main reason of favorable carbothermic reduction at considerably low temperature. However, mechanical activation of the tungstite and graphite mixtures with planetary mill for 2 h enhances the carbothermal reduction and it starts at 1000°C. The product of the carbothermal reduction was fine grained tungsten (W) with crystallite size around 50–60 nm.

Conclusions

Throughout the case studies in three different categories, importance of the charge transfer across the boundary of solid particles with dissimilar chemical species is an important common issue. Forced contact with temporal and local breakage of symmetry of crystal or ligand fields under mechanical stressing is really unique to the mechanochemical processes. As far as we use equipments with their construction more or less similar to those of grinding machine, these requirements together with constant mixing of the reactants are automatically fulfilled. For these purposes, high energy intensity is not always necessary, although there is always threshold intensity necessary for the process. The author is more than happy when some of the descriptions given above could trigger a new idea of applying mechanochemical principles to a new area of technology for innovative new processing.

Acknowledgements

The author thanks the coauthors of the case studies cited here, among others, Dr. J. G. Baek, Ms. T. Kinoshita, Dr. J. Temuujin and Ms. R. Aoyama. Some of the works were supported by COE 21, 'Life Conjugated Chemistry' program.

References

1 V. V. Boldyrev and K. Meyer, Festkörperchemie, VEB Deutscher Verlag für Grundstoffindustrie, Berlin 1973.
2 G. Heinicke, Tribochemistry, Akademie Verlag, Berlin 1984.
3 A. Z. Juhász and L. Opoczky, Mechanical Activation of Minerals by Grinding, Akadémiai Kiadó, Budapest 1990.
4 K. Tkacova, Mechanical Activation of Minerals, Elsevier, Amsterdam 1989.
5 E. M. Gutman, Mechanochemistry of Materials, Cambridge International Sci. Publ., 1998
6 P. Balaz, Extractive Metallurgy of Activated Minerals, Elsevier, Amsterdam 2000.
7 E. Avvakumov, M. Senna and N. Kosova, Soft Mechanochemical Synthesis, Kluwer Acad. Pub., New York 2001, pp. 145–166.
8 M. Senna, Solid State Ionics, 63–65 (1993) 3.
9 M. Senna, Chem. Rev., 123 (1998) 263.
10 M. Senna, Mater. Sci. Eng. A, A304–306 (2001) 39.
11 M. Senna, Ann. Chem. Sci. Mater., 27 (2002) 3.
12 M. Senna, J. Mater. Sci., 39 (2004) 4995.
13 M. Senna, Mater. Sci. Eng. A, A412 (2005) 37.
14 M. Senna, J. Eur. Ceram. Soc., 25 (2005) 977.
15 N. Tsuchiya, A. Tsukamoto, T. Oshita, T. Isobe, M. Senna, N. Yoshioka and H. Inoue, Solid State Sci., 3 (2001) 705.
16 N. Tsuchiya, A. Tsukamoto, T. Ohshita, T. Isobe, M. Senna, N. Yoshioka and H. Inoue, J. Solid State Chem., 153 (2000) 82.
17 T. Ohshita, A. Tsukamoto and M. Senna, Phys. Status Solidi A, 201 (2004) 762.
18 T. Ohshita, D. Nakajima, A. Tsukamoto, N. Tsuchiya, T. Isobe, M. Senna, N. Yoshioka and H. Inoue, Ann. Chem. Sci. Mater., 27 (2002) 91.
19 S. V. Goryainov, E. N. Kolesnik and E. Boldyreva, Physica, B – Condens. Matter, 357 (2005) 340.
20 D. Braga, L. Maini, G. de Sanctis, K. Rubini, F. Grepioni, M. R. Chierotti and R. Gobetto, Chem. Eur. J., 9 (2003) 5538.
21 A. V. Trask and W. Jones, Org. Solid State Reactions Topics, Current Chem., 254 (2005) 41.
22 H. Oguchi, C. Ando, H. Chazono, H. Kish and M. Senna, J. Phys. IV France, 128 (2005) 33.
23 C. Ando, H. Kshi, H, Oguchi and M. Senna, J. Am. Ceram. Soc., 89 (2006) 1709.
24 J. Temuujin, M. Senna, Ts. Jadambaa and D. Byambasuren, J. Metastable Nanocryst. Mater., 24–25, (2005) 581.
25 J. Temuujin, M. Senna, Ts. Jadambaa and D. Byambasuren, J. Am. Ceram. Soc., 88 (2005) 983.
26 T. Sakurai, Acta Cryst., 19 (1965) 320.
27 K. Sundaram, Int. J. Quantum Chem., 5 (1971) 101.
28 T. Sakurai, Acta Cryst., B24 (1968) 403.
29 G. G. Shipley and S. C. Wallwork, Acta Cryst., 22 (1967) 585.
30 N. B. Singh and N. N. Singh, J. Solid State Chem., 71 (1987) 530.
31 N. B. Singh and N. P. Singh, Indian J. Chem., 31 (1992) 608.
32 R. Kuroda, Y. Imai and N. Tajima, Chem. Commun., 2002 (2002) 2848.
33 E. Y. Cheung, S. J. Kitchin, K. D. M. Harris, Y. Imai, N. Tajima and R. Kuroda, J. Am. Chem. Soc., 125 (2003) 14658.
34 F. Toda, M. Senzaki and R. Kuroda, Chem. Commun., 2002 (2002) 1788.
35 H. Watanabe and M. Senna, Tetrahedron Lett., 47 (2006) 4481.
36 R. Hiraoka, H. Watanabe and M. Senna, Tetrahedron Lett., 47 (2006) 3111.
37 M. Kubinyi and G. Varasanyi, Spectrosc. Lett., 9 (1976) 689.

38 J. G. Beak, T. Isobe and M. Senna, J. Am. Ceram. Soc., 80 (1997) 973.
39 S. Komatsubara, T. Isobe and M. Senna, J. Am. Ceram. Soc., 77 (1994) 278.
40 M. Senna, T. Kinoshita, Y. Abe, H. Kishi, C. Ando, Y. Doshida and B. Stojanovic, J. Eur. Ceram. Soc., in press.
41 J. Temuujin, M. Aoyama, M. Senna, T. Masuko, C. Ando and H. Kishi, Mater. Res. Bull., in press
42 J. Temuujin, M. Aoyama, M. Senna, T. Masuko, C. Ando and H. Kishi, J. Solid State Chem., 177 (2004) 3903.
43 J. Temuujin, M. Aoyama, M. Senna, M. T. Masuko, C. Ando and C. H. Kishi, J. Mater. Res., 20 (2005) 1939.
44 M. Aoyama, J. Temuujin, M. Senna, T. Masuko, C. Ando and H. Kishi, J. Electroceram., 17 (2006) 59.
45 J. Temuujin, M. Senna, Ts. Jadambaa and D. Byambasuren, J. Metastable Nanocryst. Mater., 24–25 (2005) 581.
46 J. Temuujin, M. Senna, Ts. Jadambaa and D. Byambasuren, J. Am. Ceram. Soc., 88 (2005) 983.
47 N. J. Welham, Am. Inst. Chem. Eng. J., 46 (2000) 68.
48 G. M. Wang, S. J. Campbell, A. Calka and W. A. Kaczmarek, J. Mater. Sci., 32 (1997) 1461.
49 S. I. Cha and S. H. Hong, J. Metastable Nanocryst. Mater., 15–16 (2003) 319.

DOI: 10.1007/s10973-007-8483-z